Food Chemistry 220 (2017) 393–399

Contents lists available at ScienceDirect

Food Chemistry

journal homepage: www.elsevier.com/locate/foodchem

Analytical Methods

Utilization of spectral-spatial characteristics in shortwave infrared hyperspectral images to classify and identify fungi-contaminated peanuts

Xiaojun Qiao, Jinbao Jiang *, Xiaotong Qi, Haiqiang Guo, Deshuai Yuan

College of Geosciences and Surveying Engineering, China University of Mining and Technology, Beijing 100083, China

ARTICLE INFO

Article history:
Received 25 March 2016
Received in revised form 11 September 2016
Accepted 18 September 2016
Available online 19 September 2016

Keywords:
SWIR hyperspectral image
Fungi-contaminated peanuts
Identification
Classification

ABSTRACT

It's well-known fungi-contaminated peanuts contain potent carcinogen. Efficiently identifying and separating the contaminated can help prevent aflatoxin entering in food chain. In this study, shortwave infrared (SWIR) hyperspectral images for identifying the prepared contaminated kernels. Feature selection method of analysis of variance (ANOVA) and feature extraction method of nonparametric weighted feature extraction (NWFE) were used to concentrate spectral information into a subspace where contaminated and healthy peanuts can have favorable separability. Then, peanut pixels were classified using SVM. Moreover, image segmentation method of region growing was applied to segment the image as kernel-scale patches and meanwhile to number the kernels. The result shows that pixel-wise classification accuracies are 99.13% for breed A, 96.72% for B and 99.73% for C in learning images, and are 96.32%, 94.2% and 97.51% in validation images. Contaminated peanuts were correctly marked as aberrant kernels in both learning images and validation images.

1. Introduction

Nutrition values and the abundance of oil make the peanut a most common consumed material for edible oil, peanut butter, snacks and so on (Higgs, 2003; Yao, 2004), with the worldwide production reaching 39.42 million metric tons in 2014–2015 (USDA, 2016). However, the embarrassing fact is that during growth and storage the peanut can easily get infected with aflatoxin (AF), which is a potent carcinogen and toxic chemical produced from *A. flavus*, *A. parasiticus* or *A. nomius* (Joint FAO/WHO, 1998).

The AF family of AFB_1, B_2, G_1, G_2, M_1 and M_2 had been listed as group 1 carcinogen to human by IARC, an acronym for International Agency for Research on Cancer (IARC, 1987). Among the AFs family, the most frequent and toxic should be the subspecies of AFB_1, as appears commonly in maize or groundnuts of peanuts (Creppy, 2002; Joint FAO/WHO, 1998; McKean et al., 2006). And AFB_2 and AFG_1 even do not appear in absent of AFB_1 (IARC, 1972). AFM_1 and AFM_2 transformed from AFB_1 are generally found in milk or milk product (Bhat, Rai, & Karim, 2010), which indicates that the aflatoxin can also transfer indirectly from animals to humans. Two well-known aflatoxin outbreaks should be "Turkey X disease" and "2004 rural Kenya" whose hazardous sources are exactly from aflatoxin-contaminated peanut meal and corn (Lewis et al., 2005; Spensley, 1963). Out of consideration for food safety, approximately 100 countries have regulated their maximum tolerant limits content (MTLC) in peanut to improve peanut quality (Wu, Stacy, & Kensler, 2013).

Wet chemical methods, such as thin layer chromatography (TLC), gas chromatography (GC), and high performance liquid chromatography (HPLC), can measure the quantitative content of AFB_1, but these methods need trained laboratory personnel to conduct complex chemical operations and are time-consuming (Irineo, 2011; Wang et al., 2014). More importantly, identifying and picking out any contaminated-like peanut kernels make much sense in preventing aflatoxins entering into food chain, rather than measuring the exact quantity of AFs content. So, the urgent need is to develop a method, by which moldy or contaminated peanuts can be well identified and separated out from healthy ones, thus improving the quality of peanuts and reducing the risks of human digesting AFs.

The advent of spectroscopy imaging (or hyperspectral imaging), which acquires tens to hundred images along wavelength dimension with spatial structures shown in band-image and meanwhile spectral reflective characteristics depicted at a narrow band interval of less than 10 nm (Eismann, 2012; Robles-Kelly & Huynh, 2012). Other advantages such as no sample preparation, easiness to use, fast and nondestructive detection in practical applications

* Corresponding author.
E-mail address: jjb@cumtb.edu.cn (J. Jiang).

http://dx.doi.org/10.1016/j.foodchem.2016.09.119
0308-8146/

also make hyperspectral techniques outstanding (Burns & Ciurczak, 2007). And nowadays, hyperspectral techniques have gained impressive developments and applications in food safety and detection (Wu & Sun, 2013a).

Essentially, the qualitative identification of moldy peanuts is a binary decision in terms of the quality degree or acceptance, or rather the classification problem of pattern recognition. PCA and Discrimination analysis, such as PLS-DA (partial least square discrimination analysis) and LDA (linear discriminant analysis), should be the most frequently used method in grain quality identification (Elmasry, Kamruzzaman, Sun, & Allen, 2012). For example, Williams, Geladi, Fox, and Manley (2009) used PCA and PLS-DA to predict endosperm pixels of maize belonging to the glassy or floury. Yao et al. used LDA to identify contaminated maize as well as fungal strains from fluorescence hyperspectral images (Yao et al., 2013). Other methods for identifying grain quality mainly tend to use more advanced classifiers, such as artificial neural network (ANN) and kernel-based methods (Sun, 2010). And currently, support vector machine (SVM), which is based on kernel method, should be the most impressive and have obtained successful application in food quality identification. For example, Zhang et al. conducted classification of healthy and fungal-infected wheat kernels using support vector machine (SVM) classifier (Zhang, Paliwal, Jayas, & White, 2007). Moreover, it is very interesting to take in well-developed methods in pattern recognition to identify the agro-food quality, especially using hyperspectral techniques.

While in terms of supervised classification, there exists the contradiction between the limited training samples and the demanding for more than enough training samples to get satisfied accuracy given the high dimension of hyperspectral data, which is called the "Hughes" phenomenon (Landgrebe, 1999). The feasible choices should be: 1) using non-parametric classification models or classifiers i.e. kernel methods and SVM (Melgani & Bruzzone, 2004), sparse multinomial regression (Li, Bioucas-Dias, & Plaza, 2012) and so forth; 2) reducing the dimensionality of hyperspectral data into a subspace where various classes may have optimal separability. In this regard, linear transformations are well-used feature extraction methods to project hyperspectral features onto a lower dimensional space, such as principle component analysis (PCA), linear discrimination analysis (LDA) (Chang, 2003; Kang, Li, Fang, & Benediktsson, 2015), nonparametric weighted feature extraction (NWFE) (Kuo & Landgrebe, 2004) and so on.

In this study, fungi-contaminated peanut samples which had infected under designed storage condition were prepared. Shortwave infrared (SWIR) imaging spectroscopy at 970–2500 nm was used to acquire hyperspectral images. And the objectives of this study were to: 1) target on the spectral characteristics of fungi-contamination as well as its particular spectral responses at the wavelength range of (SWIR); 2) detect and identify the fungi-contaminated peanuts among multi-breeds to have a reliable identification method; 3) apply joint exploitation of both spectral and spatial information to identify the peanut so that the identification map can be used for future separation as in industry application.

2. Material and methods

2.1. Peanut samples preparation

Three different breeds of healthy peanuts were bought from market. Then peanut kernels with good appearance in each breed were held into containers and put into a dark and wet condition, where peanuts are easily infected with aflatoxin. In order to have clear and distinct mold, each peanut was picked out only when the kernel was fully besieged with fungus. The selected moldy peanuts were dried in a drier. Healthy kernels were chosen by hand, and furtherly checked by another two members in the experiment team to ensure they are less likely to be moldy.

2.2. Hyperspectral imaging system and image acquisition

Spectral images were acquired using a push-broom hyperspectral imaging system, HySpex SWIR-320 m-e (Norsk Elektro Optikk, 2016). The Field of View (FOV) is 13.75° with pixel FOV of 0.75 mrad. It acquires 320 pixel-wise spectra once in a line and collects spectral images in a wavelength range of 967–2499 nm with a spectral resolution of about 6 nm producing a total of 256 bands. The number of lines depends on the length of scanned object.

For each breed, peanuts were placed into four black trays with size of 10 cm × 10 cm, and two datasets of learning and validation hyperspectral images were acquired. Specifically, one tray with the kernels of all contaminated and the other with all healthy were designed as learning images. Another two trays with the peanuts kernels of some contaminated mixing among the healthy were designed as validation datasets. All trays were placed at the background of black cloth, and then the hyperspectral image was acquired. In order to perform spectral calibration, the measurements on white panel and dark current were captured simultaneously.

2.3. Hyperspectral image preprocessing

2.3.1. Spectral calibration

With the datasets of withe reflectance reference panel and dark current, pixel-wise calibration from raw detector signal intensity to reflectance was performed using with Eq. (1) (Wu & Sun, 2013b):

$$R = \frac{I_S - I_D}{I_W - I_D} \times 100\% \quad (1)$$

where R is relative reflectance of calibrated image, and R∈[0, 100]; I_S the raw hyperspectral image of samples; I_D the dark current image; and I_W the spectra of white panel.

2.3.2. Spectral smoothing

In order to reduce the random noise, a filter of moving average with the window size of 5 was adopted to smooth the spectra in a pixel-wise way. The smoothing Eq. (2) (Smith, Steven, & Colls, 2004) is as:

$$\textit{Smoothed spectrum} = \frac{1}{2.5}\left(\frac{R_{i-2}}{4} + \frac{R_{i-1}}{2} + R_i + \frac{R_{i+1}}{2} + \frac{R_{i+2}}{4}\right) \quad (2)$$

where R_i is the reflectance value of i-th band of each pixel, and i∈[3, 254].

2.3.3. Image background removal

Non-peanut pixels were masked as background with the value of zero, and they can be easily separated due to its reflectance far below than peanuts. Furthermore, Morphology corrosion processing was applied to reduce the influence of mixed pixels at kernel edge. Other data preprocessing includes image resizing.

2.4. Data processing and analysis

2.4.1. Feature selection and extraction

It's true that numerous channels of hyperspectral images provide more chances to identify and differentiate materials. However, with regard to a specific scenario of hyperspectral image, these bands have different ability for material separation (Chang, 2007). In addition, hyperspectral image contains a large amount of redundant information. Thus band selection and extraction is

necessary to both save useful bands for further application and avoid computation burden as well as the 'Hughes' phenomenon. In this study, one-way ANOVA was firstly adopted to quantitatively estimate the separability in each band between fungi-contaminated and healthy classes. The 95% confidence level ($p < 0.05$) was adopted to retain the effective bands and to remove the bands with poor separability.

Among the feature extraction methods in hyperspectral images, NWFE is shown to outperform others in classification (Kuo & Landgrebe, 2004). NWFE is also based on linear projection transformation like PCA. However, the projection direction of NWFE is obtained via sample distribution instead of variance matrix in PCA (Chang, 2007). Therefore, NWFE is used in this study to get the transformation direction, where the fungi-contaminated and healthy training samples are anticipated to have preferable separability, and then the hyperspectral image was projected.

From the above, the feature selection and extraction methods used in this study are as follow: Firstly the bands with $p > 0.05$ are removed due to their poor separability; Secondly, top rank bands with larger F values in ANOVA were selected out for classification, and the number of top-rank bands is determined by cross validation of training samples with maximum accuracy; Thirdly, the retained bands with $p < 0.05$ are projected using NWFE transformation; Finally, the NWFE feature and top-F bands are stacked together as feature set for further classification.

2.4.2. Pixel-wise classification with SVM

Based on the stacked features above, kernel methods and SVM were adopted to classify peanut pixel as the fungi-contaminated or healthy. To be specific, kernel trick firstly maps the features into a higher feature space, where classes can be separated easily, and then optimal hyperplane that maximums the margin are determined by SVM according to the distribution of training samples (Richards, 2013). SVM can get satisfied accuracy in hyperspectral classification even when there are limited training samples, and is free of parameter estimation. And Gaussian Radial Basis Function (RBF) kernel SVM classifier was adopted in this study.

2.4.3. Image spatial segmentation using region growing

There are two objectives of segmentation. The first is to smooth noise-like misclassified pixels whose labels have distinct difference with the surroundings. The second is to give each kernel patch a serial number so as to decide if the kernel was moldy enough for further separation.

Anomaly of digital signal sampling, mixed pixels, spectra variability and among others, can lead to misclassification in remote sensing. Thus, a single peanut kernel can't be determined as contaminated if there are only few contaminated pixels in a healthy kernel, and vice versa. To avoid this, a ratio threshold is adopted in this study. In detail, kernels will be determined as aberrant when the ratio of fungi pixel number to total pixel number exceeds the threshold of β. Finally, with the segmented map, fungi-contaminated peanut kernels can be easily tracked according to their serial number.

To this end, a binary image, which was composed of 0 for background and 1 for peanut, was firstly obtained; and then the region growing algorithm with 4-neighborhood was used to connect pixels within the same kernel patch and assign a serial number.

2.4.4. Flow-chart of image processing

To better clarify the image processing steps, the flow chart is shown as in Fig. 1. In particular, the dashed line section is specific for learning images to determine optimal wavebands and projection vector in NWFE. Validation images skip the dashed line section and used the wavebands and the vector same as the learning images.

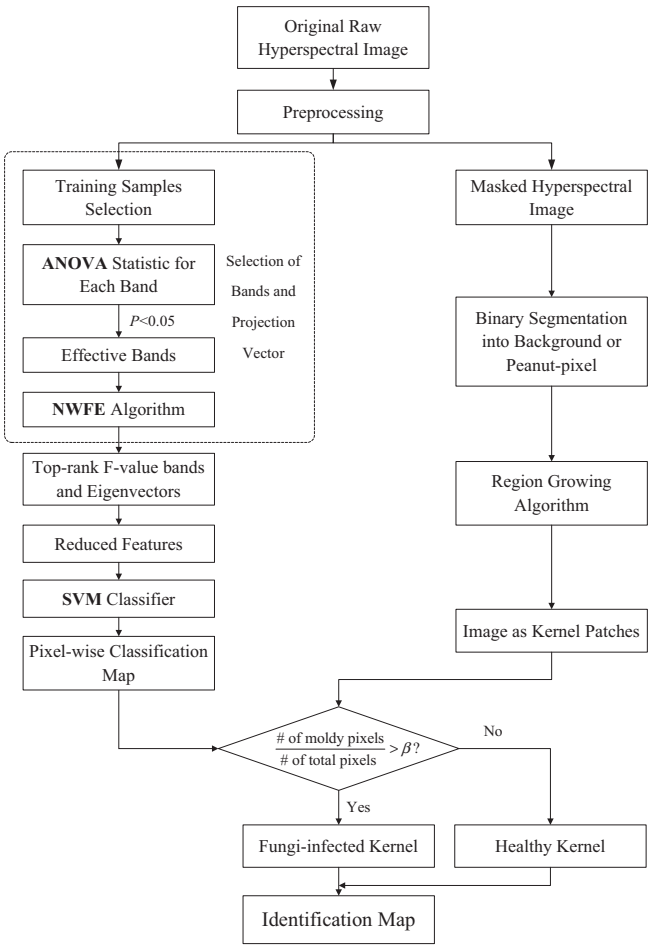

Fig. 1. The flow-chart of hyperspectral image processing and main steps.

Except for NWFE, all the data processing procedures were performed in Matlab R2010a (The MathWorks Inc.), ENVI 4.8 (Exelis Visual Information Solutions, Boulder, CO, USA), and ArcGIS 10 (Environmental Systems Research Institute, Inc.). And the NWFE was conducted in MultiSpec image analysis system (Biehl & Landgrebe, 2002).

3. Result and discussion

3.1. Feature selection and extraction

Considering the moldy kernel was almost all contaminated, pixels of training samples were chosen randomly in each kernel. And training samples in healthy peanuts were obtained likewise. In detail, twenty pixels were firstly selected randomly from each kernel, and then visual check was followed to remove training pixels with uncertainty of being healthy or contaminated. Final training samples included 1864 contaminated pixels and 1840 healthy, and the rest pixels were treated as testing samples. In order to have knowledge of the spectral response, mean spectra of the fungi-contaminated training samples as well as the healthy were calculated in each of the three breeds, as shown in Fig. 2. As a whole, the mean reflectance of fungi-contaminated peanuts was lower than that from the healthy peanuts in the wavelength range of 967–1153 nm and higher in the wavelength range of 1400–2500 nm, which are distinct spectral response features for identification. Twenty bands (1153 nm ~ 1183 nm and 1231 nm ~ 1309 nm) whose probabilities are bigger than

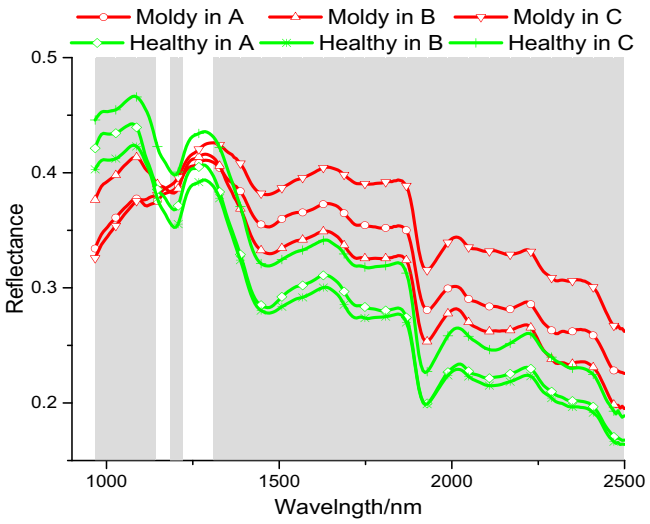

Fig. 2. Effective bands selection with ANOVA statistic.

0.05 were removed shown as white background wavelengths in Fig. 2. The retained effective bands were fed to the NWFE algorithm to get optimal projection vector. And then the NWFE-feature was obtained by projecting the hyperspectral image. Five-fold cross validation of training samples was used to determine the number of top-rank F-value bands with the maximum accuracy. Finally, Top 17 bands of 1916, 1922, 1910, 1928, 1934, 1904, 1940, 2493, 1946, 2475, 1898, 2499, 1952, 2487, 2469, 1958 and 2451 nm were in candidate and were stacked together with NWFE-feature for further classification.

3.2. Classification results in learning images

All the training samples characterized by the stacked features were used to choose optimal parameters in kernel function and to train SVM classifier. SVM classification was implemented using LIBSVM (Chang & Lin, 2011) and the optimal parameters of C and γ in RBF were determined by five-fold cross validation, giving: $C = 100$, $\gamma = 0.25$. With the trained SVM classifier and optimal parameters of C and γ, testing samples in learning images were classified. In Fig. 3, the training samples were marked in white color to highlight the labels of testing samples. As can be seen from Fig. 3, the classification results in learning images are close to truth with the distribution of left for the contaminated and right for the healthy. The quantitative accuracies are 99.13%, 96.72% and 99.73% respectively as in Table 1. Then, whether a kernel was contaminated was decided by the ratio of fungi-contaminated pixel number to total pixel number without

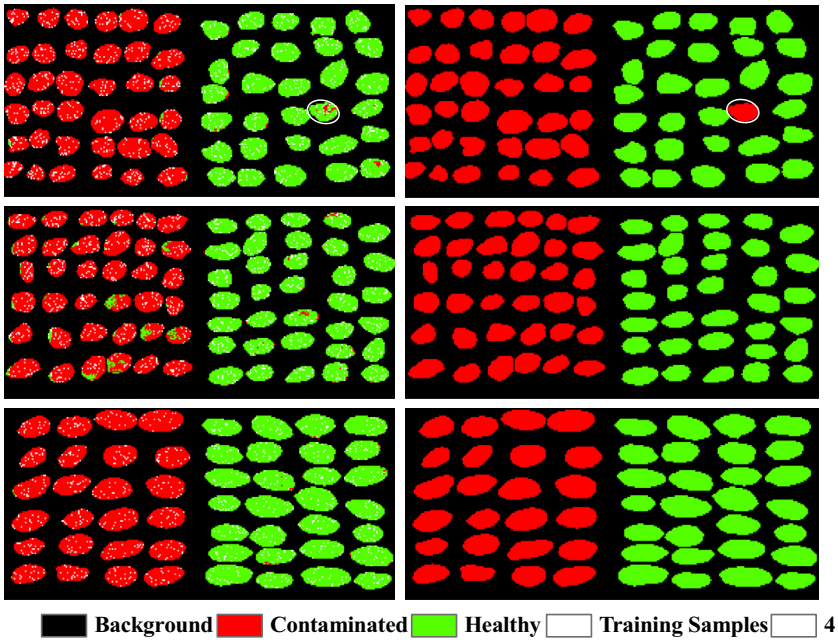

Fig. 3. Classification result in learning image with the left column for pixel-wise classification and the left for kernel-scale identification map; pictures in each row for breed A, B and C from up to down; the bottom giving the legend.

Table 1
Classification result in learning images.[#]

Breeds	True classes	Pixel-wise classification		Kernel-scale identification		Overall accuracy	
		Contaminated	Healthy	Contaminated	Healthy	Pixel-wise	Kernel-scale
A	Contaminated	5934	29	37	0	99.13%	98.70%
	Healthy	74	5849	1	29		
B	Contaminated	5317	306	36	0	96.72%	100%
	Healthy	67	5678	0	34		
C	Contaminated	6320	4	24	0	99.73%	100%
	Healthy	34	7933	0	28		

[#] Unit with the "pixel" in pixel-wise classification and the "kernel" in kernel-scale identification.

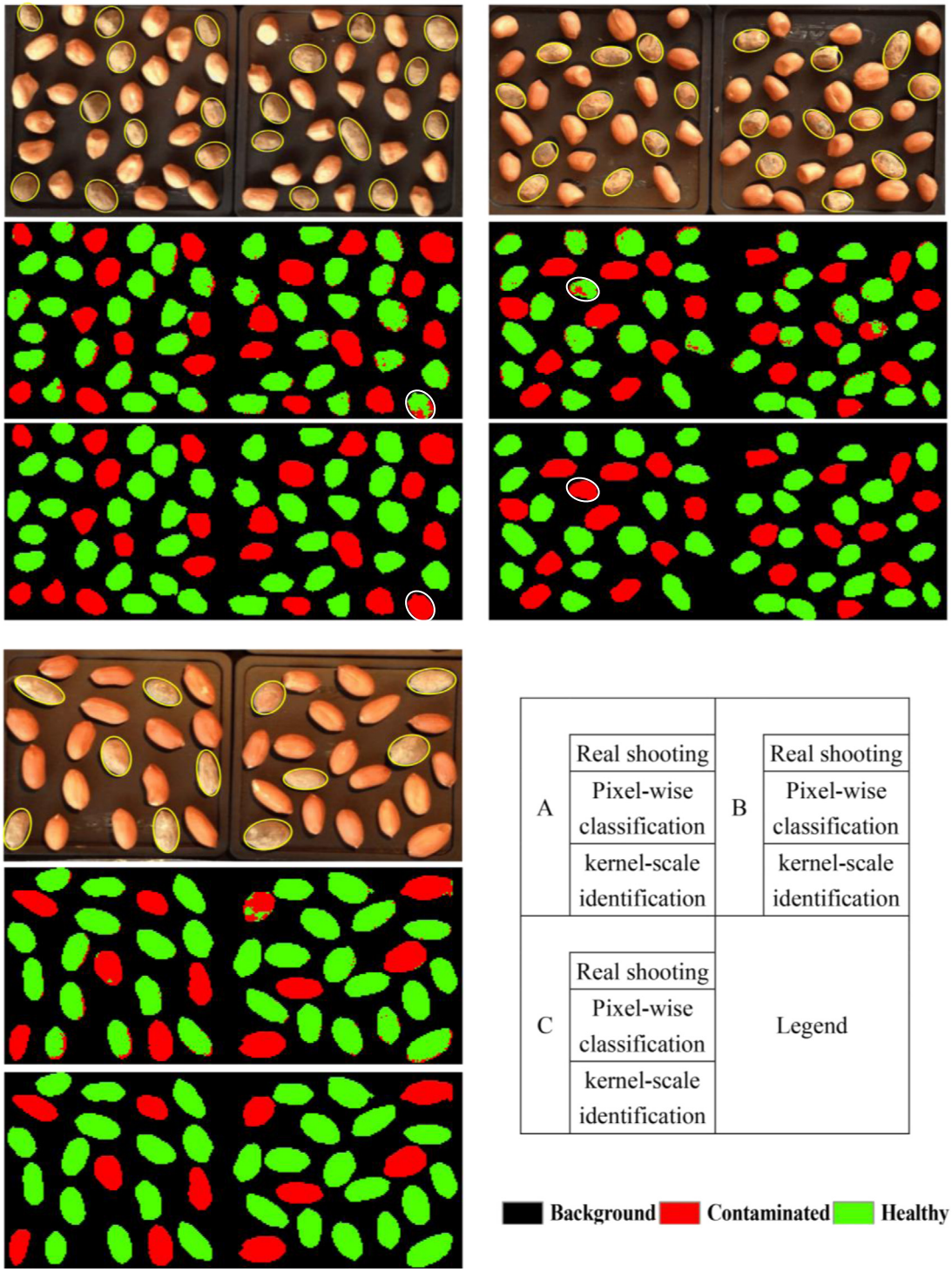

Fig. 4. Classification results in validation images; real shooting, pixel-wise classification and kernel-scale identification images in each breed were group from top to bottom as illustrating with the legend at the bottom right of the figure; capital letters of A, B, and C correspond to the breed name.

calculating the training pixels. If the ratio is bigger than some threshold of β as 0.15 in this study, the kernel should be treated as fungi-contaminated. The reasons for choosing β = 0.15 are that: 1) the small threshold is just used for ignoring some misclassified pixels in each kernel; 2) the small threshold can decline uncertain kernels, thus improving the quality of peanuts in practical production.

In order to give a comparative estimation of the proposed method, the well-used method of PCA followed by PLS-DA were conducted to have pixel-wise identification accuracies. In detail, training samples were same as in the learning images. All bands were fed to PCA for feature reduction, and first 3 PCs were retained for further PLS-DA classification. The result gave 94.47%, 90.53% and 96.02% for breed A, B and C respectively. Compared with the accuracies, it is obvious that the proposed method in this study obtained better results. Although PLS-DA is good enough, better trained classifier is more desirable so as to be applied in practical detection.

Table 2
Classification result in validation images.[#]

Breeds	True classes	Pixel-wise classification		Kernel-scale identification		Overall accuracy	
		Contaminated	Healthy	Contaminated	Healthy	Pixel-wise	Kernel-scale
A	Contaminated	3912	20	10	0	96.32%	98.25%
	Healthy	404	7178	1	46		
B	Contaminated	3261	7	10	0	94.20%	98.15%
	Healthy	570	6101	1	43		
C	Contaminated	3192	76	11	0	97.51%	100%
	Healthy	226	8615	0	30		

[#] Unit with the "pixel" in pixel-wise classification and the "kernel" in kernel-scale identification.

3.3. Classification results in validation images

The validation images with the distribution of few contaminated kernels mixing among the healthy were classified using the trained classifier and parameters in learning images. Classification results are shown as in Fig. 4 and Table 2. The pixel-wise classification maps in Fig. 4 indicate satisfactory result with most pixels classified correctly except for some mixed pixels at kernel margins. Table 2 gives the pixel-wise classification accuracies of 96.32% for breed A, 94.20% for B and 97.51% for C. Although there exists some misclassified pixels, reconsidering the quality of each peanut at a kernel-scale spatially can smooth them and give reliable decision of whether a kernel is fungi-contaminated. More importantly, kernel-scale identification maps can clearly tell which peanut is contaminated and should be separated.

However, it should be pointed out that three healthy kernels were "wrongly" identified as the contaminated using the threshold $\beta = 0.15$, which is out of accord with in-kind shooting pictures as in Figs. 3 and 4. The reasons may be as following: 1) contaminated pixels of the three "wrongly" identified kernels have the chance of being getting moldy; 2) slightly contaminated peanuts could be normal to human eyes, but they do have aberrant spectral response. This is exactly the strengths of SWIR hyperspectral imaging seeing objects at broader wavelength range far beyond visible. Furthermore, it is preferable to rigorously decline any contaminated-like kernels rather than to easily accept them. However, it must be pointed out that chances are that threshold β can inevitably bring in detecting false negatives, which is unacceptable because some moldy pixels can accepted as healthy. Again, it is suggested that the threshold β should be as small as possible.

4. Conclusion

Both healthy and moldy peanuts showed distinct spectral response for identifying the moldy at the wavelength range of SWIR. This study classified and identified the contaminated pixels in a framework of hyperspectral classification, which obtained the accuracies no less than 94% in both learning images and validation images. The proposed methods were validated with validation images from a perspective of on-line detection, which showed satisfied performance. More importantly, contaminated kernels were told in result map, which is significant for industry application in tracking and separating the aberrant kernels. It should be pointed out that although three breeds of peanuts were collected in this study, identifying multifarious fungi-contaminated peanuts is still anticipated in the framework of classification, based on well-trained classifiers and typical library of training samples. Further works will continue to include peanuts with more breeds, different shapes as broken, and various appearances as fractured. With enriched library of moldy knowledge and well-trained classifier, contaminated peanuts can be easily separated in practical application. Another, more factors need to be considered, such as moisture content and oil content, so as to have more reliable and effective methodology for moldy-peanuts identification in industry.

Acknowledgements

The research was sponsored by National Natural Science Foundation of China (41571412).

References

Bhat, R., Rai, R. V., & Karim, A. A. (2010). Mycotoxins in food and feed: present status and future concerns. *Comprehensive Reviews in Food Science and Food Safety, 9*(1), 57–81.

Biehl, L., & Landgrebe, D. (2002). MultiSpec—a tool for multispectral–hyperspectral image data analysis. *Computers & Geosciences, 28*(10), 1153–1159. Software available at https://engineering.purdue.edu/~biehl/MultiSpec/hyperspectral.html.

Burns, D. A., & Ciurczak, E. W. (Eds.). (2007). *Handbook of near-infrared analysis* (3rd ed.. Boca Raton, FL, USA: CRC Press.

Chang, C. I. (2003). *Hyperspectral imaging: techniques for spectral detection and classification* (Vol. 1). Springer Science & Business Media.

Chang, C. I. (Ed.). (2007). *Hyperspectral data exploitation: theory and applications*. John Wiley & Sons.

Chang, C. C., & Lin, C. J. (2011). LIBSVM: A library for support vector machines. *ACM Transactions on Intelligent Systems and Technology (TIST), 2*(3), 27.

Creppy, E. E. (2002). Update of survey, regulation and toxic effects of mycotoxins in Europe. *Toxicology Letters, 127*(1), 19–28.

Eismann, M. T. (2012). *Hyperspectral remote sensing*. Bellingham: SPIE.

Elmasry, G., Kamruzzaman, M., Sun, D. W., & Allen, P. (2012). Principles and applications of hyperspectral imaging in quality evaluation of agro-food products: A review. *Critical Reviews in Food Science & Nutrition, 52*(11), 999–1023.

Higgs, J. (2003). The beneficial role of peanuts in the diet-Part 2. *Nutrition & Food Science, 33*(2), 56–64.

IARC. (1972). Some inorganic substances, chlorinated hydrocarbons, aromatic amines, N-nitroso compounds, and natural products. IARC Monographs on the Evaluation of the Carcinogenic Risk of Chemicals to Man, 1.

IARC (1987). *Overall evaluations of carcinogenicity: An updating of IARC monographs volumes 1 to 42*. International Agency for Research on Cancer: World Health Organization.

Irineo, Torres-Pacheco (Ed.). (2011). *Aflatoxins – Detection, measurement and control, agricultural and biological sciences*. InTech.

Joint FAO/WHO Expert Committee on Food Additives (JECFA) (1998). Aflatoxins: Safety evaluation of certain food additives and contaminants. In *The Forty-Ninth Meeting of the Joint FAO/WHO Expert Committee on Food Additives, WHO Food Additive Series no. 40* (pp. 359–468). Geneva, Switzerland: World Health Organization. http://www.inchem.org/documents/jecfa/jecmono/v040je16.htm.

Kang, X., Li, S., Fang, L., & Benediktsson, J. A. (2015). Intrinsic image decomposition for feature extraction of hyperspectral images. *IEEE Transaction on, Geoscience and Remote Sensing, 53*(4), 2241–2253.

Kuo, B. C., & Landgrebe, D. A. (2004). Nonparametric weighted feature extraction for classification. *IEEE Transaction on, Geoscience and Remote Sensing, 42*(5), 1096–1105.

Landgrebe, D. (1999). Information extraction principles and methods for multispectral and hyperspectral image data. *Information Process Remote Sensing, 82*, 3–38.

Lewis, L., Onsongo, M., Njapau, H., Schurz-Rogers, H., Luber, G., Kieszak, S., et al. (2005). Aflatoxin contamination of commercial maize products during an outbreak of acute aflatoxicosis in eastern and central Kenya. *Environmental Health Perspectives, 113*(12), 1763–1767.

Li, J., Bioucas-Dias, J. M., & Plaza, A. (2012). Spectral–spatial hyperspectral image segmentation using subspace multinomial logistic regression and Markov

random fields. *IEEE Transactions on, Geoscience and Remote Sensing, 50*(3), 809–823.
McKean, C., Tang, L., Tang, M., Billam, M., Wang, Z., Theodorakis, C. W., & Wang, J. S. (2006). Comparative acute and combinative toxicity of aflatoxin B 1 and fumonisin B 1 in animals and human cells. *Food and Chemical Toxicology, 44*(6), 868–876.
Melgani, F., & Bruzzone, L. (2004). Classification of hyperspectral remote sensing images with support vector machines. *IEEE Transactions on, Geoscience and Remote Sensing, 42*(8), 1778–1790.
Norsk Elektro Optikk (2016). <http://www.hyspex.no/products/disc/swir-320m-e.php>.
Richards, J. A. (2013). Remote sensing digital image analysis. An introduction fifth edition. Heildelberg
Robles-Kelly, A., & Huynh, C. P. (2012). *Imaging spectroscopy for scene analysis*. Springer Science & Business Media.
Smith, K. L., Steven, M. D., & Colls, J. J. (2004). Use of hyperspectral derivative ratios in the red-edge region to identify plant stress responses to gas leaks. *Remote Sensing of Environment, 92*(2), 207–217.
Spensley, P. C. (1963). Aflatoxin, the active principle in turkey 'x' disease. *Endeavour, 22*, 75–79.
Sun, D. W. (Ed.). (2010). *Hyperspectral imaging for food quality analysis and control*. Elsevier.
USDA (2016). <http://apps.fas.usda.gov/psdonline/psdreport.aspx?hidReportRetrievalName=BVS&hidReportRetrievalID=918&hidReportRetrievalTemplateID=1>.
Wang, W., Heitschmidt, G. W., Ni, X., Windham, W. R., Hawkins, S., & Chu, X. (2014). Identification of aflatoxin B_1 on maize kernel surfaces using hyperspectral imaging. *Food Control, 42*, 78–86.
Williams, P., Geladi, P., Fox, G., & Manley, M. (2009). Maize kernel hardness classification by near infrared (nir) hyperspectral imaging and multivariate data analysis. *Analytica Chimica Acta, 653*(2), 121–130.
Wu, F., Stacy, S. L., & Kensler, T. W. (2013). Global risk assessment of aflatoxins in maize and peanuts: Are regulatory standards adequately protective? *Toxicological Sciences, 135*(1), 251–259.
Wu, D., & Sun, D. W. (2013a). Advanced applications of hyperspectral imaging technology for food quality and safety analysis and assessment: A review—part II: Applications. *Innovative Food Science & Emerging Technologies, 19*, 15–28.
Wu, D., & Sun, D. W. (2013b). Advanced applications of hyperspectral imaging technology for food quality and safety analysis and assessment: A review—Part I: Fundamentals. *Innovative Food Science & Emerging Technologies, 19*, 1–14.
Yao, G. (2004). Peanut production and utilization in the People's Republic of China. Peanut in Local and Global Food Systems Series Report, 4.
Yao, H., Hruska, Z., Kincaid, R., Brown, R. L., Bhatnagar, D., & Cleveland, T. E. (2013). Detecting maize inoculated with toxigenic and atoxigenic fungal strains with fluorescence hyperspectral imagery. *Biosystems Engineering, 115*(2), 125–135.
Zhang, H., Paliwal, J., Jayas, D. S., & White, N. D. G. (2007). Classification of fungal infected wheat kernels using near-infrared reflectance hyperspectral imaging and support vector machine. *Transactions of the ASABE, 50*(5), 1779–1785.